Journal of Catalysis **202,** 141–155 (2001)
doi:10.1006/jcat.2001.3266, available online at http://www.idealibrary.com on IDEAL®

A DFT Study of Isomerization and Transalkylation Reactions of Aromatic Species Catalyzed by Acidic Zeolites

Xavier Rozanska,*,[1] Xavier Saintigny,* Rutger A. van Santen,* and François Hutschka†

*Schuit Institute of Catalysis, Laboratory of Inorganic Chemistry and Catalysis, Eindhoven University of Technology, P.O. Box 513, 5600 MB Eindhoven, The Netherlands; and †TotalFinaElf, Centre Européen de Recherche et Technique, Département Chimie des Procédés, B.P. 27, 76700 Harfleur, France

Received February 8, 2001; accepted April 18, 2001

A theoretical study of the isomerization and transalkylation reactions of aromatic species catalyzed by acidic zeolite is reported. Cluster DFT calculations have been performed. All different reported mechanisms of isomerization and transalkylation have been investigated and analyzed. The aromatic species considered in this study are benzene, toluene, and alkylated thiophene and derivatives. © 2001 Academic Press

Key Words: **Brønsted acid site; zeolite; DFT calculations; quantum chemistry; transition state; isomerization; transalkylation; aromatics.**

1. INTRODUCTION

Isomerization and transalkylation reactions of alkylated aromatics are some of the most important petrochemical processes (1). Acidic zeolite catalysts are used to catalyze these reactions (2). They present the advantage that they can be applied at higher temperature as solid acids. Their micropores present opportunities for stereochemical control of selectivity (3).

In this paper we will provide a full investigation of the elementary reaction steps that constitute the catalytic cycle of these reactions. We will report on the isomerization and transalkylation reactions of toluene. This molecule can be seen as a small-scale model of other larger aromatics (4). Moreover, petrochemical feedstock contains heteroaromatic species, such as alkylated thiophenic species (5). We will also describe reaction paths and their corresponding reaction energy diagrams of isomerization and transalkylation of some thiophene derivatives. Thiophene has been reported to show similar electrophilic properties as toluene (1a, 6).

First, we will consider intramolecular isomerization or unimolecular isomerization reactions of toluene, methylthiophene, and thiophenic derivatives. Then, we will study intermolecular or bimolecular transalkylation of toluene with benzene and thiophene.

We used the cluster approach method to complete a full analysis of the different reactions of intra- and intermolecular isomerization. The catalytic active site, viz. the Brønsted acidic site, is modeled in this method by a small fragment that has similar activity than acidic zeolite active site (7). This method has been used for many years and has been shown to be a relevant approach for reaction energy diagram investigations (8–10). A four-tetrahedral cluster ($Al(OHSiH_3)(OSiH_3)_2(OH)$) has been chosen.

However, the absence of the micropore zeolitic structure around the Brønsted acidic site and reaction molecule may lead to substantial differences between cluster results and the actual behavior in the zeolites (11, 12). Especially, such a model cannot describe the interaction between the reactive system and zeolite wall. Consequently, intermediate and transition state geometries obtained with such an approach are free of any steric constraints and therefore correspond to ideal geometries that potentially can be adopted within zeolite micropore. Moreover, zeolite framework electrostatic contributions are absent from this model. Zeolite micropores have been shown to have a stabilizing effect on the carbocationic transition states with respect to gas phase results, which can be on the order of 10 to 30% of the activation energies (12). This stabilization has been demonstrated to be of short range electrostatic nature (12b). Boronat *et al.* (13a) or Sinclair *et al.* (13b) have shown that the effect of electrostatic stabilization originating from the zeolitic structure on transition states is uniform. So, one expects that for our calculations the activation energies will be overestimated but that the qualitative trends will be conserved. We did not use constraints on the geometry of the small cluster as recommended before (10c, 14).

As the zeolite catalyst is only modeled by a Brønsted acid site, adsorption energies computed here do not correspond to adsorption energies within the zeolite micropore. All energy contributions of the molecule interacting with atoms of the zeolite wall are missing. Therefore the adsorption

[1] To whom correspondence should be addressed. Fax: +31 40 245 5054. E-mail: tgakxr@chem.tue.nl.

0021-9517/01 $35.00

energies we present only describe the affinity of molecules for the Brønsted acid site. It has been discussed elsewhere how to correct empirically for these adsorption energies in real zeolites (4, 15, 16).

2. METHODS

"Gaussian98" (17) has been used for the calculations with the density functional method B3LYP (18). This DFT method is a hybrid method that uses a Hartree–Fock core and a Becke exchange functional with the correlation functionals developed by Lee *et al.* (18). Zygmunt *et al.* (19) have shown that this method is the best choice for DFT treatment of zeolite cluster systems, and they present results comparable with MP2 method.

We selected the basis set d95: we have shown in a previous study that this basis set gives reasonable basis set superposition error (BSSE) (20). The basis set superposition correction has been checked on intermediates and transition states using the counterpoise method (21). On intermediate geometries the BSSE is below 7 kJ/mol, and on activation energies it is below 11 kJ/mol.

Geometry optimization calculations have been carried out to obtain local minima for reactants, adsorption complexes and products, and to determine the saddle point for transition states (TS). Frequency calculations have been computed in order to check that the stationary points exhibit the proper number of imaginary frequencies: none for a minimum and one for a transition. Zero point energy (ZPE) corrections have been calculated for all optimized structures. All energies presented are zero point energies, unless stated.

3. RESULTS AND DISCUSSION

3.1. Monomolecular Mechanism

We will report here the different reaction paths and the reaction energy schemes of monomolecular isomerization (or intramolecular isomerization) of toluene and alkylated thiophene derivatives.

3.1.1. Toluene

The toluene isomerization reaction study is important to define clearly the reaction paths. This molecule constitutes an efficient small-scale model of larger systems, such as poly-alkylated benzene or derivatives (*viz.* poly-alkylated benzothiophene derivatives) (4). The small-size of this system allows full investigations of different reaction pathways. These investigations led to the identification of two alternative mechanistic routes.

Shift 1-2 isomerization. Toluene is protonated and its methyl shifts from C_α to C_β in this reaction. Then, the exceeding proton is back-donated to the acidic site. This reaction has been demonstrated to occur in acidic homogeneous catalysis chemistry as well as zeolite catalysis chemistry (4, 22–24).

Actually, with acidic zeolite catalyst, the detailed reaction path followed is different from the path that occurs in homogeneous catalysis. Acidic zeolite catalysts are known to induce reactions similar to those obtained with superacids (25). Gorte (26) or Haw *et al.* (27) demonstrated that this is in fact not the case at the elementary reaction step level. Whereas superacids have high dielectric constant and show strong solvatation effects, zeolite catalysts present characteristics similar to gas phase systems (26, 28) with dielectric constants close to vacuum constants (29). Earlier findings (29a, 30) support these claims. Charged intermediates in zeolites cannot be considered as stable intermediates but as part of transition state structure (31).

After toluene adsorption on the acidic proton ($E_{\text{ads}} = -20$ kJ/mol), the protonation step occurs. The zeolite proton attacks the toluene C_α atom (see Fig. 1 and Scheme 1). Such a mechanism leads to the formation of a stable Wheeland complex intermediate in super-acids (25). Charged species separation presents however a too high-energy cost within a zeolite (7a). It has been demonstrated experimentally (27a) and theoretically (31a) that an alkoxy bond is formed between a Lewis basic oxygen atom and C atom of reactant to stabilize the formation of protonated species. A similar result is found for toluene.

The activation energy barrier of toluene protonation and phenoxy species formation is $E_{\text{act}} = 201$ kJ/mol. The phenoxy species, which is the product of the reaction, is computed to be less stable than adsorbed toluene ($\Delta E = 152$ kJ/mol). With conditions required to achieve this reaction (22–24), one may assume that experimentally this intermediate has a short residence time (2, 27a). The adsorbed Wheeland complex geometry has also been checked. All geometry optimizations lead either to the phenoxy species or to adsorbed toluene.

When the phenoxy species O–C bond stretches, the species evolves toward a Wheeland complex and toluene reaches its isomerization transition state structure. The activation energy barrier of the shift 1-2 isomerization step is $E_{\text{act}} = 282$ kJ/mol with respect to adsorbed toluene. The protonation or backdonation step does not happen at this stage. We performed a constrained geometry optimization to get an order of magnitude of the charged complex energy level. The cluster geometry as in the transition state mechanism step has been kept fix and put in presence of a fully free protonated toluene. It is well known that the geometry of a zeolitic Al–O–Si unit changes considerably whether the bridging oxygen atom is protonated or not (7a, 9b). The constraints on the Al–O–Si angles prohibit the proton back-donation. The constrained optimized geometry optimization gives energy of 240 kJ/mol with respect to adsorbed toluene for the charged species. This is not a stable

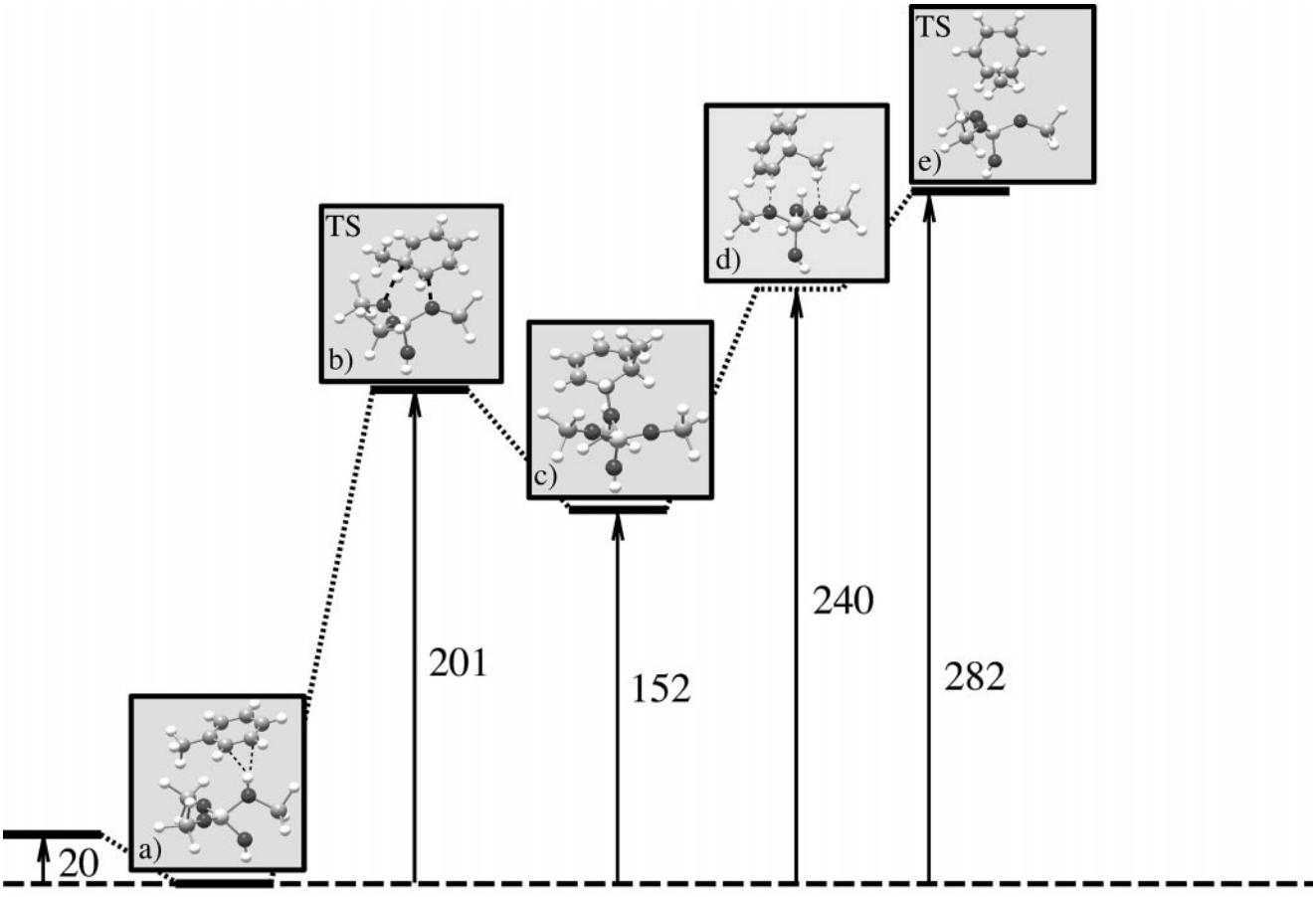

FIG. 1. Reaction energy diagram and geometries of the intermediates and transition states for the shift 1–2 mechanism isomerization reaction of toluene catalyzed by acidic zeolite (data in kJ/mol).

system, and a full optimization of this geometry leads to a phenoxy species.

The shift 1–2 isomerization reaction may be decomposed into three distinct parts (see Scheme 1). Initially, toluene is protonated in an activation step. This step depends on proton acidity. It is the only step where the proton is explicitly involved.

Isomerization via the disproportionation reaction. Disproportionation via the methyl alkoxy mechanism of the isomerization reaction of toluene has been shown to occur within acidic zeolite (23). Again, as for the shift 1–2 isomerization reaction of toluene, the aromatic molecule is first protonated. This protonation step leads to a phenoxy species as earlier described (see Fig. 1). When phenoxy is released from the cluster, the reaction pathway follows the same reaction chain as that for the shift 1–2 mechanism reaction. But a different transition state structure is reached. The charged toluene species can lose its methyl group. The disproportionation structure geometry is shown in Fig. 2. Toluene transfers its methyl to the benefit of a Lewis basic oxygen atom. The activation energy barrier of this reaction is $E_{act} = 279$ kJ/mol with respect to adsorbed toluene. The products of this reaction are benzene and methyl alkoxy (see Fig. 2). This intermediate energy level is 70 kJ/mol above absorbed toluene energy. Benzene may desorb from the methyl alkoxy species. The adsorption energy is only $E_{ads} = -5$ kJ/mol. It can therefore easily desorb and move away from the methyl alkoxy. It has been demonstrated recently that methyl alkoxy may be used as an active site to achieve reactions (20).

The computed maximum activation energy step of this reaction is within less than 3 kJ/mol the same as the activation barrier energy of the shift 1–2 isomerization mechanism (E_{act} are 279 and 282 kJ/mol, respectively). No transition state selectivity should be expected for one or the other of the monomolecular reaction pathways. Both of them require the same activation barrier energy (∼280 kJ/mol) and both of them involve a transition state of the same size (see Scheme 1). Further consideration of the activation entropy indicates a slightly more favorable situation for the isomerization via methyloxy intermediate (see Table 1).

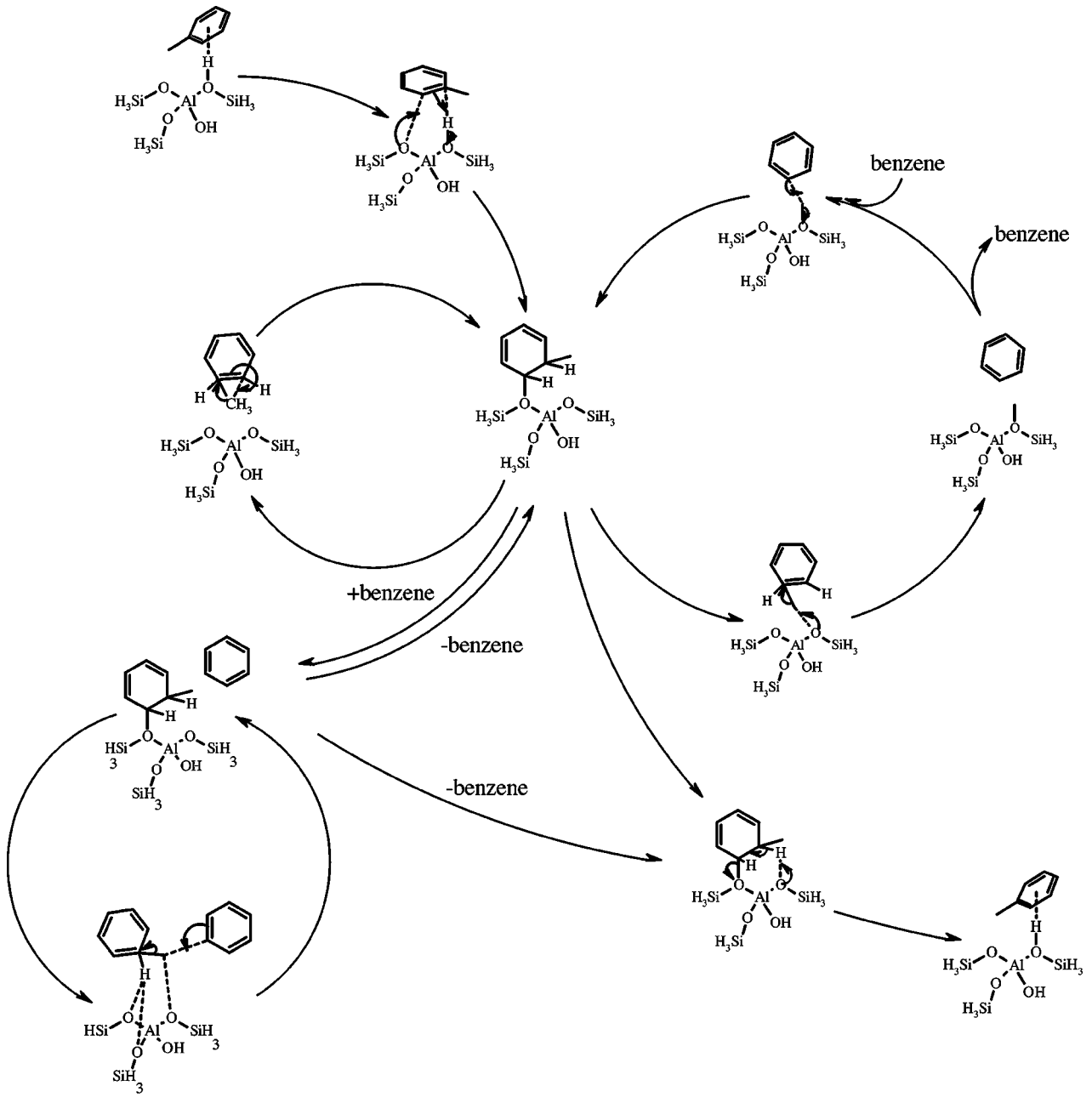

SCHEME 1. Catalytic cycles of isomerization and transalkylation reactions of toluene and benzene. Initiation step is the attack of the proton on C_α.

3.1.2. Thiophene Derivatives

Alkylated thiophene derivatives are more difficult to desulfurize than their nonalkylated equivalents (5, 32). Especially, the yield of hydrodesulfurization reaction decreases dramatically in the case of 46DMDBT (see Scheme 2) (33). Several authors assumed that for this compound, the methyl groups prevent the sulfur atom to be in contact with the catalytic active site. It is now well accepted that the use of bifunctional catalysts, composed of a classical desulfurization catalyst component (34) and an acidic zeolite catalyst, increases by a factor 3 the desulfurization rate (5). Michaud *et al.* (32) have reported that the 46DMDBT hydrodesulfurization product does indeed correspond to the product reached from its isomer (viz. 36DMDBT), which shows a less hidden sulfur atom. They proposed that isomerization of dimethyldibenzothiophene occurs prior to desulfurization.

First, monoalkylated thiophenes will be studied. These compounds are less easily desulfurized than nonalkylated species. Then the methyl benzothiophene isomerization reaction will be considered.

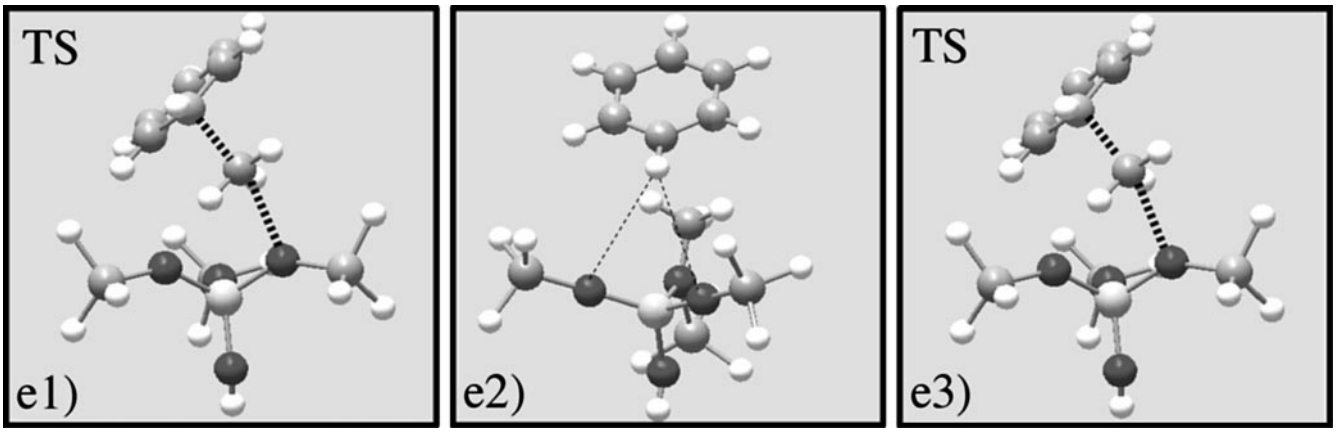

FIG. 2. Geometries of the intermediate (e2) and transition states (e1 and e3) of the disproportionation via methyl alkoxy mechanism isomerization reaction of toluene.

Methyl thiophene. As in the case of monomolecular isomerization of toluene, the methyl–thiophene isomerization may proceed following two different pathways, viz. the shift mechanism isomerization and the disproportionation mechanism pathway (mediated via methyl alkoxy). We will limit this study to the methyl-1-thiophene to methyl-2-thiophene isomerization reactions.

The shift mechanism and the disproportionation mechanism of methyl-thiophene compounds are similar to the toluene mechanisms. They need both an initial protonation step that leads to the formation of σ-bonded ions (or thiophenoxy species), from which the isomerization step takes place. This isomerization reaction step constitutes the limiting step of the reaction.

The reaction energy diagram and geometries of the shift mechanism isomerization of methyl-(1,2)-thiophene are shown in Fig. 3. Methyl-1-thiophene and methyl-2-thiophene adsorb on the cluster via a η^1(S) adsorption mode to the acidic proton, in agreement with the IR study of the adsorption of thiophene within acidic zeolite performed by Lercher *et al.* (35). The adsorption energies of methyl-1-thiophene and methyl-2-thiophene on the cluster

TABLE 1

Computed Thermodynamic Data of the Reactions

Reaction	Figure(s)	Reaction step	$\Delta_{298}G^{\#}$(kJ/mol)	$\Delta_{298}H^{\#}$(kJ/mol)	$\Delta_{298}S^{\#}$(J/mol/K)
Isomerization of toluene	1	a→e	287	283	−13
Isomerization of toluene	1 and 2	a→e1	280	282	7
	2	e2→e1	219	213	−17
Isomerization of methyl-thiophene	3	a→d	254	239	−50
	3	g→d	262	240	−76
Isomerization of methyl-thiophene	3 and 4	a→d1	255	250	−16
	4	d2→d1	184	184	2
	4	d2→d3	206	206	−2
	3 and 4	g→d3	286	272	−46
Isomerization of methyl-benzothiophene	5	a→d	285	269	−53
	5	g→d	276	266	−33
Transalkylation toluene–benzene	7	d1→d2	298	292	−21
Transalkylation toluene–benzene	1 and 8	a→b	305	298	−23
	8	d→e	175	168	−25
	8	f→e	232	225	−22
Transalkylation toluene–thiophene	1 and 10	a→e1	297	274	−79
	1 and 10	a→e2	300	278	−73
	3 and 10	a→e1	297	276	−69
	3 and 10	g→e2	285	281	−11
	1 and 11	a→e	302	277	−86
	4 and 11	d2→h	197	196	−3

Note. All data are reported for a temperature of 298 K.

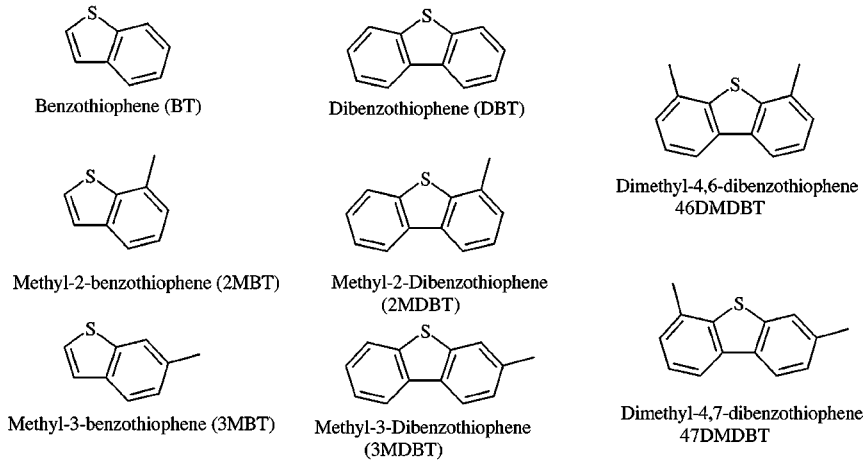

SCHEME 2. Some thiophenic derivatives.

are respectively $E_{ads} = -18$ and -19 kJ/mol. The protonation of methyl-1-thiophene on its C_α position (C_1 atom) appears to occur with an activation barrier energy 38 kJ/mol lower than the methyl-2-thiophene energy ($E_{act} = 119$ and 157 kJ/mol respectively). Geobaldo *et al.* (6) reported that the preferred protonation position of thiophene within the acidic zeolite is the C_1 position.

Methyl-1-thiophene protonation reaction step results in a methyl-thiophenoxy species 8 kJ/mol lower than the methyl-thiophenoxy species formed in the case of methyl-2-thiophene.

As for toluene, the shift methyl-thiophene isomerization mechanism can be described as the shifting of a methyl cation from a carbon atom to another. The cluster participates to the mechanism only via the stabilizing effect of the methyl carbenium by the Lewis basic oxygen atoms. The activation energy barrier that is required to achieve isomerization step of methyl-1-thiophene is

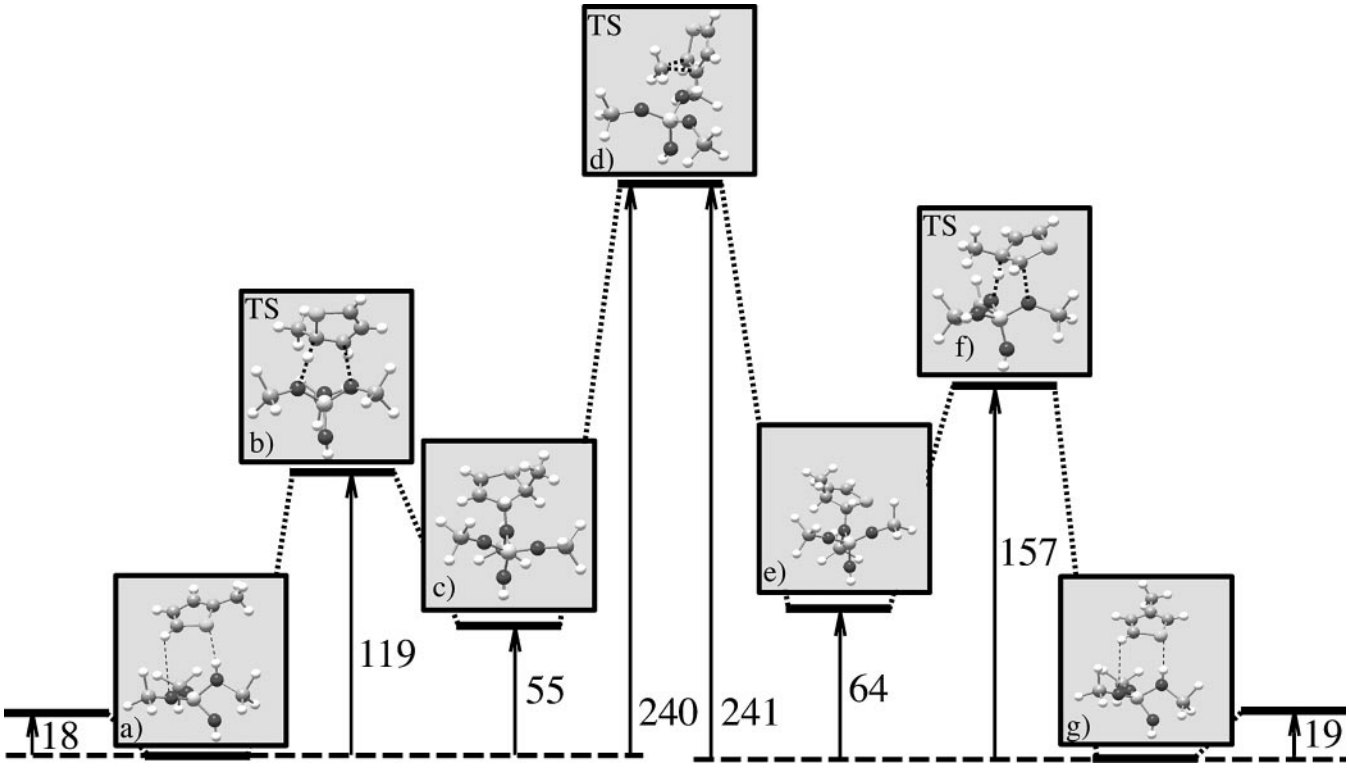

FIG. 3. Reaction energy diagram and geometries of the intermediates and transition states for the shift 1–2 mechanism isomerization reaction of methyl thiophene(data in kJ/mol).

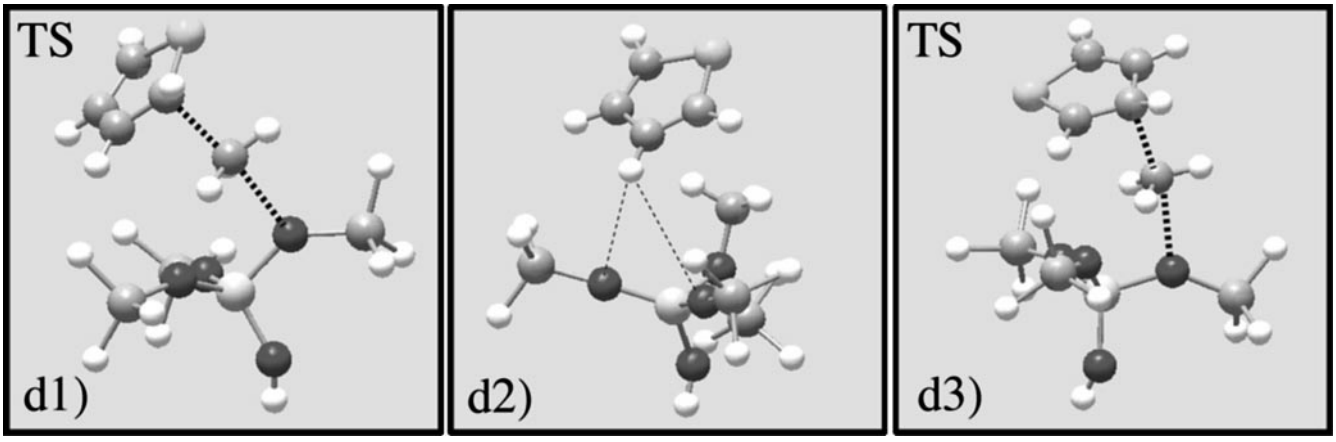

FIG. 4. Geometries of the intermediate (d2) and transition states (d1 and d3) of the isomerization reaction of methyl–thiophene via the disproportionation reaction.

$E_{act} = 240$ kJ/mol. It is 241 kJ/mol for methyl-2-thiophene (see Fig. 3).

The isomerization reaction can also occur through the breaking of the bond between thiophene and the methyl group, and consecutive formation of a bond between the methyl group and a Lewis basic oxygen atom (disproportionation mechanism) (see Fig. 4). The initiation step that allows this transition state is the same the previous step (see Fig. 3). The disproportionation transition state structures are energetically different for the two isomers: the computed activation energy barriers show an energy difference of 22 kJ/mol. As for the proton attack mechanism, the methylation in the C_2 position gives a higher energy barrier ($E_{act} = 250$ and 272 kJ/mol for methyl-1-thiophene and methyl-2-thiophene, respectively). After this reaction has occurred, thiophene adsorbs to a methyl alkoxy species. Thiophene is not strongly physisorbed to the methyl alkoxy. The adsorption energy is only −5 kJ/mol. For methyl-1-thiophene and methyl-2-thiophene formation thiophene and methyl alkoxy undergo methylation of thiophene with $E_{act} = 181$ and 202 kJ/mol, respectively.

The highest activation energy barrier for the shift mechanism isomerization is $E_{act} = 241$ kJ/mol. For the disproportionation mechanism isomerization this is $E_{act} = 272$ kJ/mol. One may assume that the isomerization reaction of methyl-thiophene follows preferentially the shift mechanism isomerization pathway.

Methyl benzothiophene. The isomerization of methylbenzothiophene has also been studied. For this compound, only the shift mechanism of isomerization has been investigated. Its reactivity is actually more closely related to toluene than to alkylated thiophene (see Fig. 5). However, energy differences between toluene and 2MBT isomerization exist and will be reported.

The adsorption energies of 2MBT and 3MBT (see Scheme 2) are $E_{ads} = -20$ kJ/mol. An activation barrier energy of $E_{act} = 192$ kJ/mol is required to overcome the barrier of the proton attack and thiophenophenoxy species formation mechanism step for 2MBT. The thiophenophenoxy species energy level is +137 kJ/mol above the adsorbed 2MBT. The proton attack activation energy barrier is $E_{act} = 205$ kJ/mol in the case of 3MBT. The phenoxy species is +177 kJ/mol with respect to adsorbed 3MBT.

After protonation, isomerization can be achieved. The transition state geometry is close to that of toluene. The activation barrier energy is $E_{act} = 270$ kJ/mol with respect to adsorbed 2MBT. This barrier is 12 kJ/mol smaller than the shift isomerization activation energy barrier of toluene.

The shift isomerization mechanism transition states of 4MDBT and 46DMBT have been also computed (see Fig. 6). However, adsorption geometries have not been computed because of the large size of these molecules. Interactions with the molecules and the hydrogen atoms of the SiH_3 groups cannot be avoided. These interactions do not have physical meaning, as such SiH_3 groups do not exist in zeolite catalyst. Transition states geometries of isomerization of 4MDBT and 46DMDBT are very similar to the toluene and 2MBT geometries (see Fig. 6). As the adsorption geometries could not be defined we used instead the activation energy barriers of the gas phase systems as reference. Activation energies with respect to the gas phase systems are 262, 250, 250, and 248 kJ/mol for the shift mechanism isomerization transition states of toluene, 2MBT, 4MDBT, and 46DMBDT, respectively.

3.2. Bimolecular Mechanisms

3.2.1. Toluene–Benzene

The reaction steps of the transalkylation reaction between toluene and benzene will be analyzed. These reactions allow also the isomerization of toluene. Moreover, they can also be considered as model reactions of

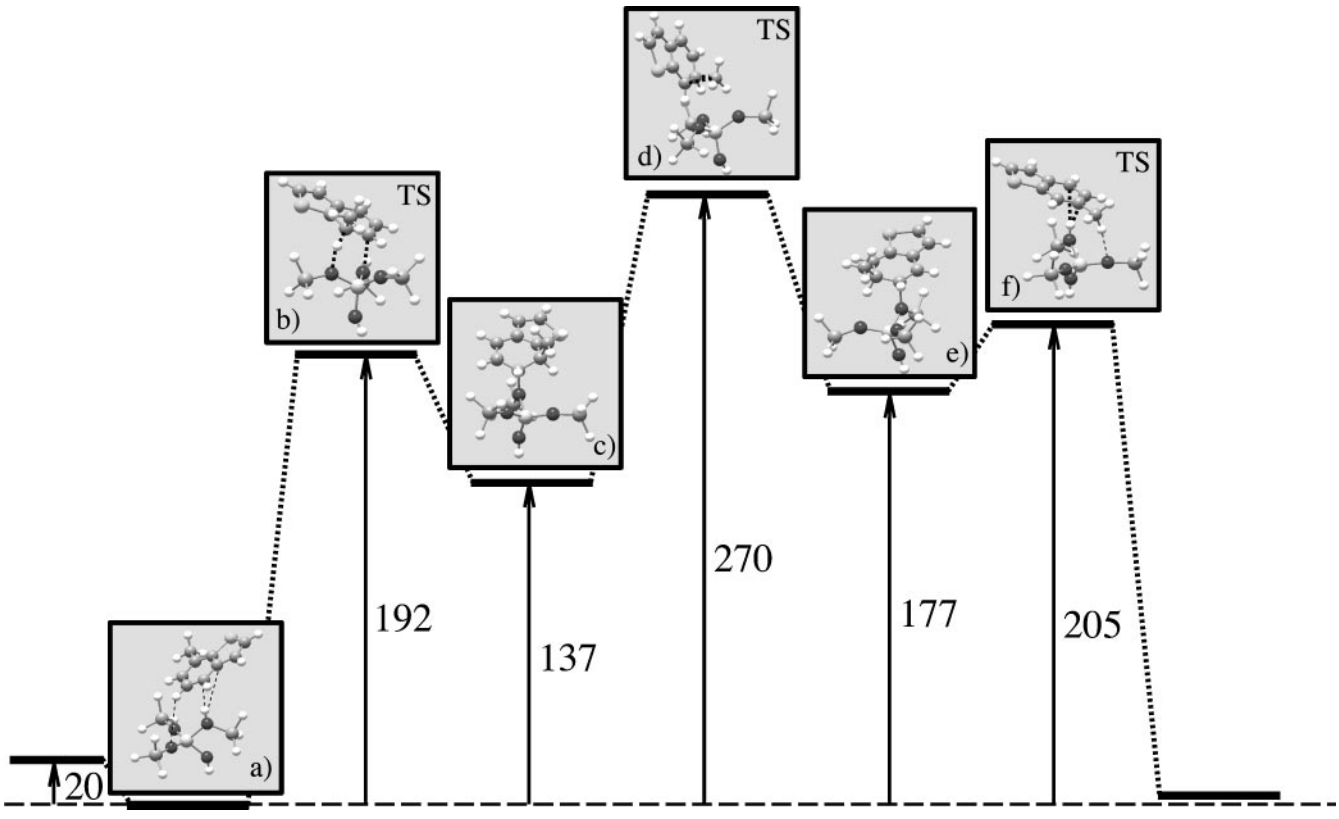

FIG. 5. Reaction energy diagram and geometries of the intermediates and transition states of the shift 1–2 mechanism isomerization reaction of M2BT (data in kJ/mol).

transalkylation reactions between toluene molecules that lead to the formation of xylenes and benzene (23, 24, 36, 37). Toluene worldwide production is more important than the actual needs (38) and the transformation of this low valuable molecule in higher valuable molecules, viz. benzene and xylenes, is of interest. Two mechanisms of transalkylation have been proposed. Transalkylation may occur via a direct transalkylation reaction between toluene and benzene, with an exchange of a methyl group. It has been also proposed that this reaction proceeds through a diphenylmethane intermediate (36). We will investigate both mechanisms.

The direct transalkylation mechanism. Interestingly, the initiation step of this reaction sequence is the same as the initiation step of the shift reaction as well as disproportionation reaction of isomerization (see Fig. 1). Toluene must be activated prior to the transalkylation mechanism. This occurs via the proton attack and phenoxy formation mechanism previously described. We computed the corresponding transition state in the presence and absence of benzene. The presence of benzene does not help the reaction. The difference of activation energies between the two transition states is less than 5 kJ/mol. Benzene can be considered absent for the initiation step. It adsorbs on the alkoxy species (see Fig. 7). This physisorbtion is very weak with $E_{ads} = -3$ kJ/mol. The alkoxy desorbs from the Lewis basic oxygen atom and then reacts with benzene (see Fig. 7). The activation energy barrier for the transalkylation mechanism is $E_{act} = 277$ kJ/mol. The hydrogen atom that comes from the acidic site is not in interaction with a Lewis basic oxygen atom. This shows that the protonation–transalkylation–proton backdonation mechanism does not occur in a single mechanistic step (associative mechanism) but in several mechanistic steps (consecutive mechanism).

The activation energy of the transalkylation mechanism is the same as the activation energies of the isomerization mechanisms ($E_{act} = 277$ kJ/mol and for shift and disproportionation isomerization mechanisms 279 and 282 kJ/mol, respectively). Since energetically no difference in energy is predicted, and because transalkylation is bimolecular reaction, it is expected to be more favored as monomolecular isomerization reactions as long as micropore sizes do not prevent formation of the large transition state (37) (see Scheme 1).

The diphenylmethane intermediate mechanism. This mechanism has been proposed to be the dominant one within large pore zeolite (1–4, 36–38). The first step of this mechanism is believed to be the attack of the acidic proton

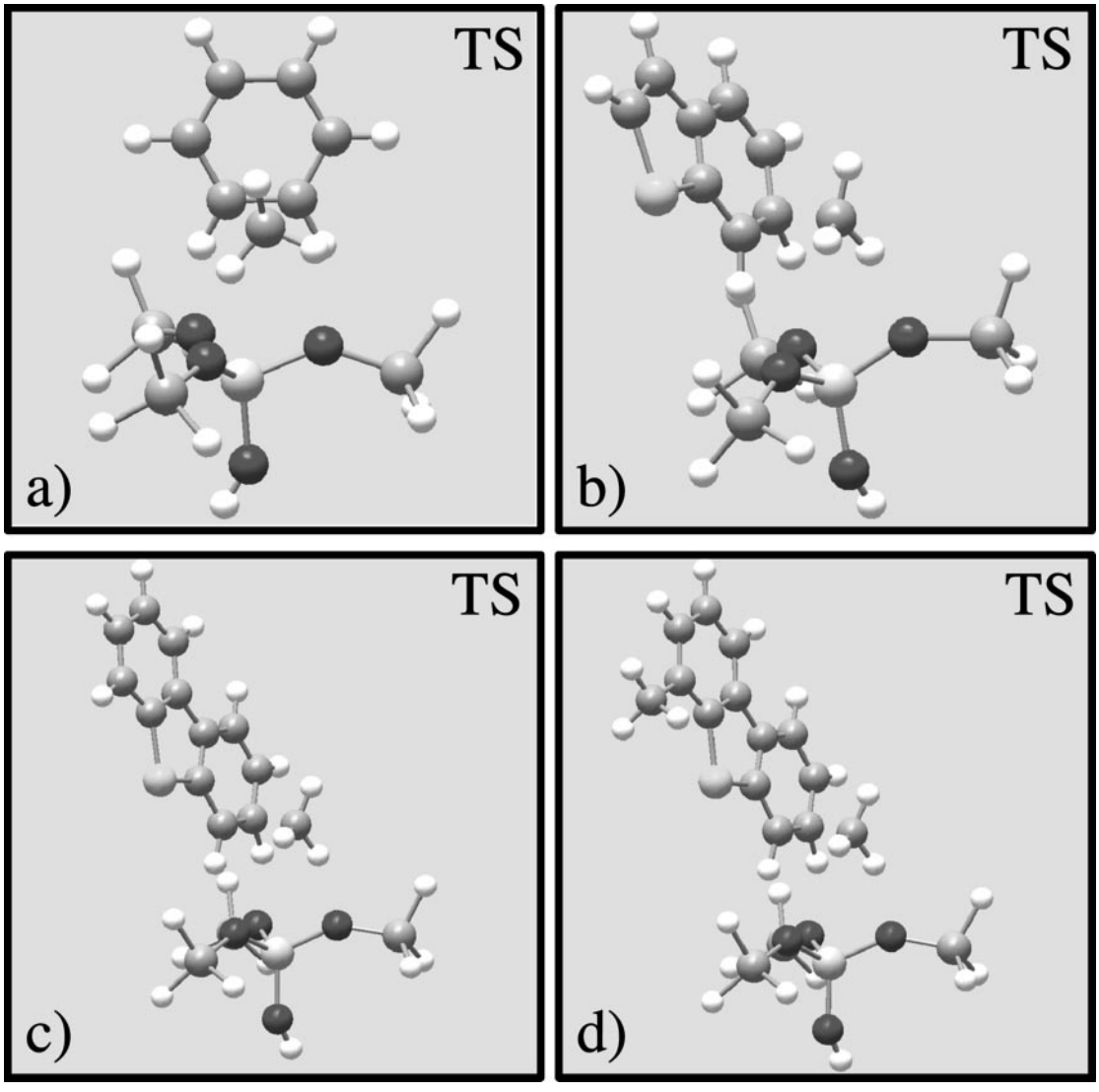

FIG. 6. Geometries of the transition states for the shift isomerization reactions of (a) toluene, (b) MBT, (c) MDBT, and (d) DMDBT.

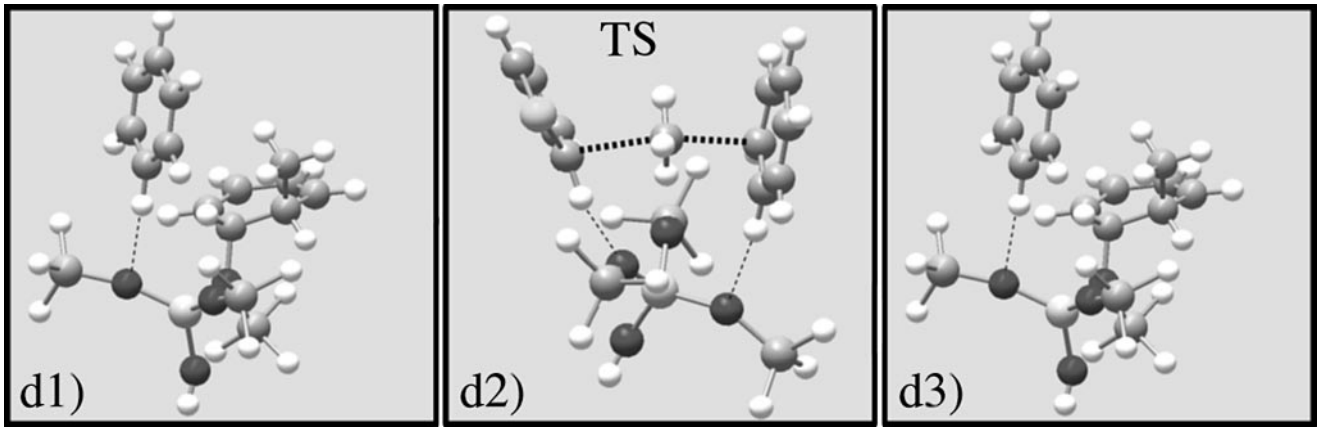

FIG. 7. Geometries of the intermediates (d1 and d3) and transition state (d2) for the transalkylation between toluene and benzene via the direct mechanism.

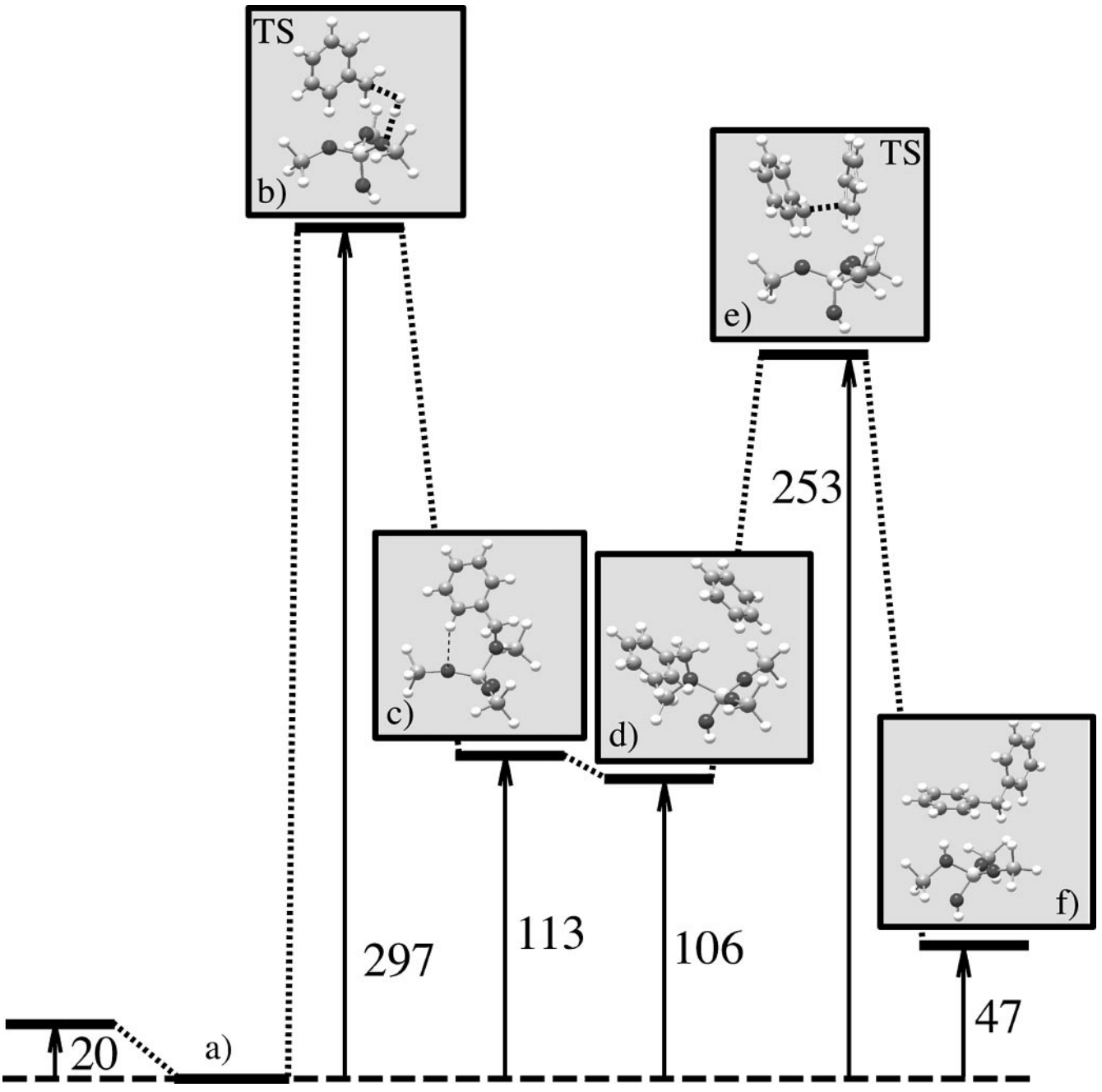

FIG. 8. Reaction energy diagram and geometries of the intermediates and transition states of the transalkylation reaction between toluene and benzene via diphenylmethane (data in kJ/mol).

on the methyl group of toluene in order to form H_2 and a benzyl carbenium ion. Of course charged species cannot be stabilized by the zeolite long-range electrostatic contribution and we found a slightly different reaction pathway to be followed. The geometries of intermediates and transition states of this transalkylation via diphenylmethane intermediate mechanism are shown in Figs. 8 and 9.

The initiation transition state mechanism step leads to the formation of H_2 and benzyl alkoxy species. H_2 desorbs quickly from the acidic site. The activation energy barrier of this reaction step is relatively high ($E_{act} = 297$ kJ/mol). The back reaction is considerably more difficult than in the case of the previous proton attack on the C_α of toluene ($E_{act} = 49$ kJ/mol for direct transalkylation back mechanism and $E_{act} = 184$ kJ/mol for the present). Morin *et al.* (24b) and Guisnet *et al.* (38) suspected that the active sites for this reaction are more acidic than the sites for isomerization reaction. Benzyl alkoxy evolves quickly because it is relatively

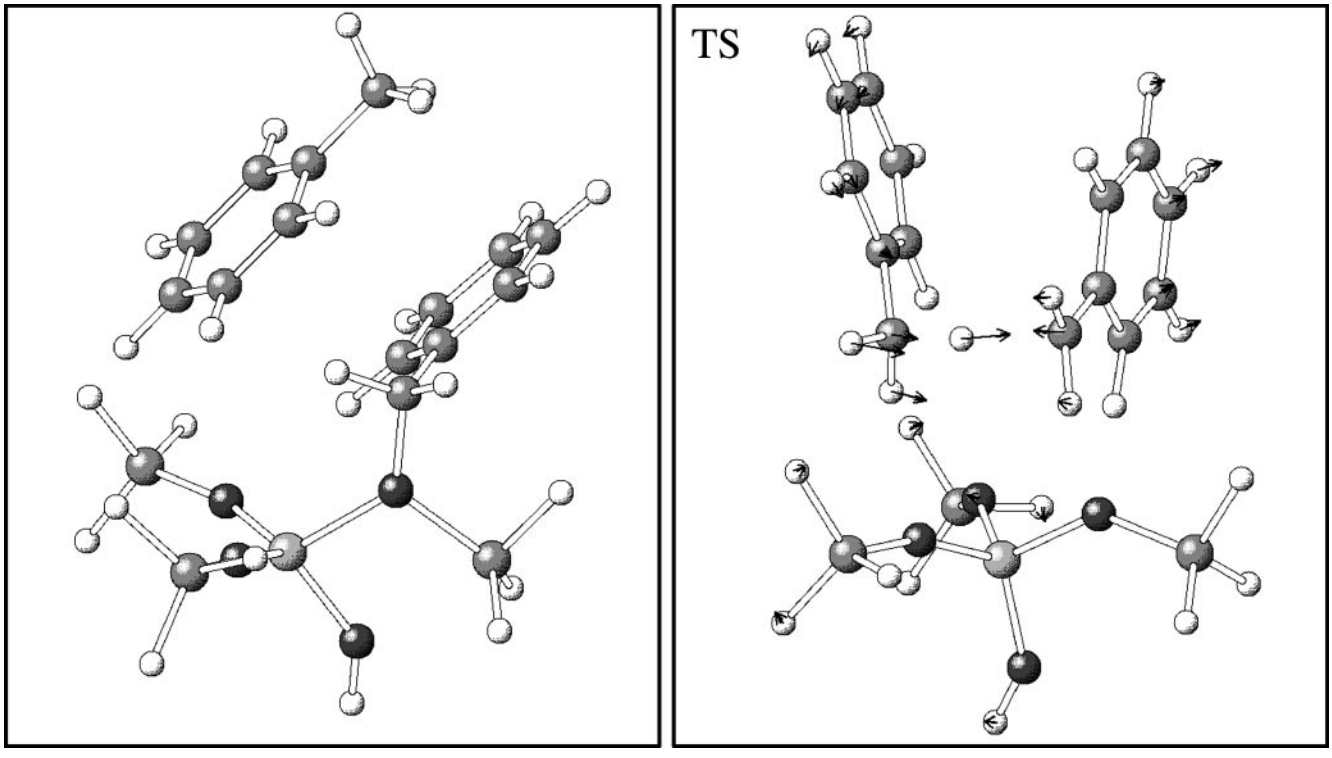

FIG. 9. Geometries of the intermediate (left) and transition state (right) of the hydrid transfer reaction between toluene and benzyloxy.

unstable to another species (its energy level is 113 kJ/mol with respect to adsorbed toluene). Benzene can adsorb nearby (E_{ads} is only -7 kJ/mol). Then, the diphenylmethane formation reaction can occur. The corresponding transition state activation energy barrier is $E_{act} = 148$ kJ/mol with respect to benzene adsorbed on benzyl alkoxy and 253 kJ/mol with respect to toluene adsorbs on the cluster and benzene. The benzyl alkoxy is released from the Lewis basic oxygen atom, and benzene attacks the C_1 carbon atom and forms a diphenylmethane molecule. The proton back-donation to the cluster is a consecutive mechanism to this transition state and occurs without activation energy. Diphenylmethane adsorbed to the acidic proton is 47 kJ/mol less stable than adsorbed toluene and benzene. The back-reaction has a low barrier. Benzene and toluene are formed. Uncertainties exist at this stage whether the methyl group will stay on its parent aromatic ring or is exchanged to the benefit of the other aromatic ring. Steric constraints and diffusion of the products drive the reaction to the formation of some selective isomers in zeolite micropores. However, once initiated this mechanism is less susceptible to be deactivated than direct transalkylation mechanism and the catalytic cycle may be continued (see Scheme 3). Alternatively, hydrid transfer reaction can take place between the benzyloxy intermediate and a toluene molecule (see Fig. 9). This mechanism allows another toluene to get involved in the catalytic cycle. The activation energy barrier of the hydrid transfer mechanism is 286 kJ/mol with respect to 2 toluene molecules adsorbed to the acidic site. The initiation step activation energy is $E_{act} = 297$ kJ/mol. The activation energy of the hydrid transfer reaction is $E_{act} = 178$ kJ/mol with respect to toluene adsorbed on benzyloxy intermediate ($\Delta_{298K}H_{act}$ and $\Delta_{298K}G_{act}$ are 179.3 and 185.1 kJ/mol, respectively).

Despite the lower activation energies, this mechanism has been reported to present other difficulties (37). Two effects exist that cannot be estimated by DFT study. First, H_2 can deactivate the catalytic cycle. H_2 is required for the termination step. But it is helpful in preventing coke formation and consecutive deactivation of catalytic active sites. Moreover, relatively large size intermediates are mandatory in this mechanism. Zeolite micropore size is a crucial parameter to allow for this mechanism to occur. Morin *et al.* (24b) have shown that partial deactivation of active sites first affect the stronger acidic sites. The mechanism of transalkylation via diphenylmethane intermediate will be immediately affected. Furthermore, they shown that rate of this mechanism decreases more quickly that the one of isomerization reaction due to coke formation.

3.2.2. Toluene–Thiophene

We will study the transalkylation reaction between toluene and thiophene in this part. We will limit the investigation to the direct transalkylation mechanism but will check the different possibilities of methylating positions

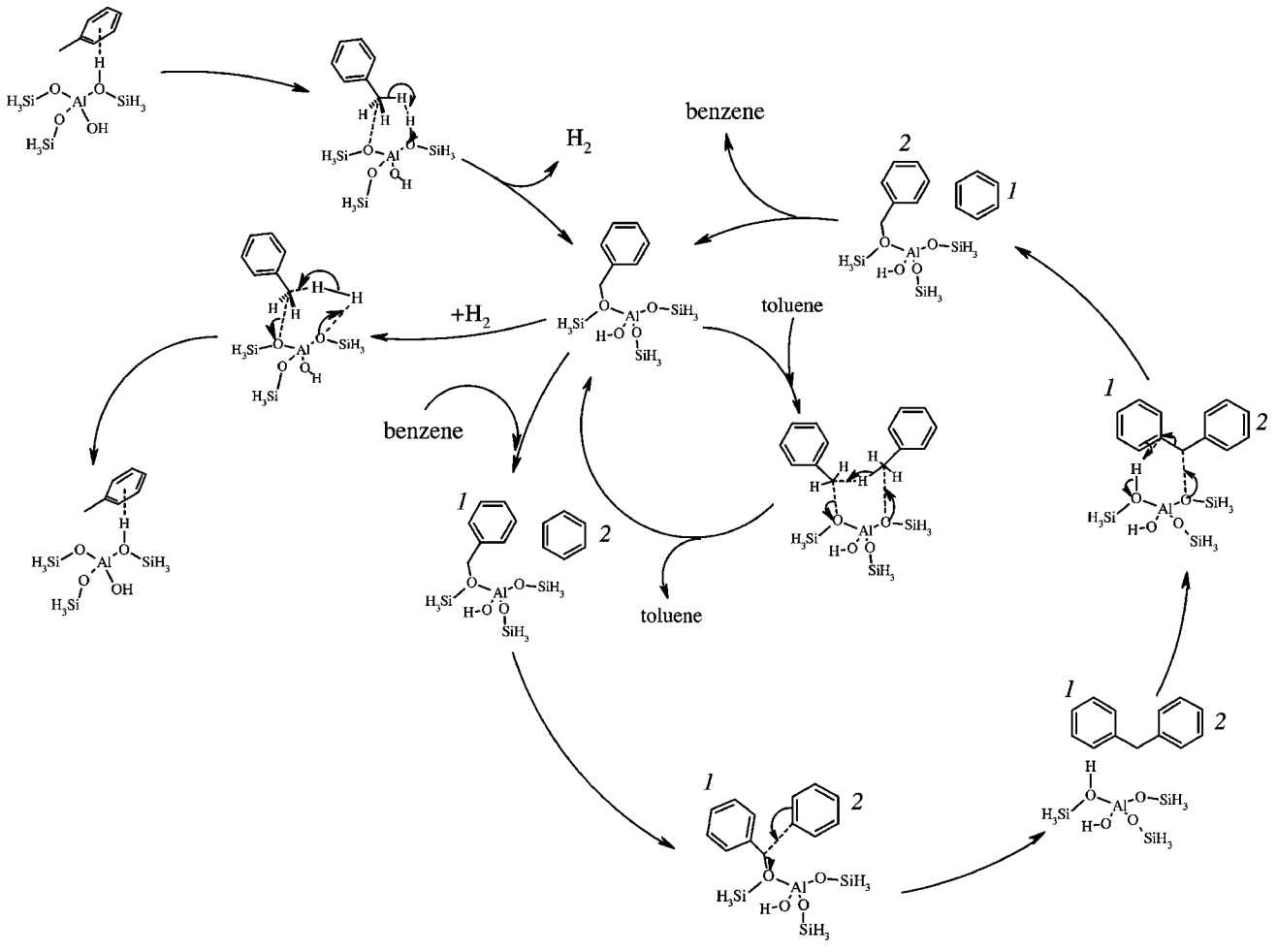

SCHEME 3. Catalytic cycles of transalkylation reaction of toluene and benzene via the diphenylmethane intermediate. Initiation step is a proton attack on the hydrogen atom of the toluene methyl group that leads to the formation of H_2.

on thiophene. The alkylation reactions between alkylated thiophenes and benzene present the double advantage of inducing a decrease of benzene content in gas-oil (39), and a formation of more easily desulfurized thiophenic species (5, 32, 35a).

The first step of this reaction pathway is the attack of the acidic proton on toluene that undergoes formation of the toluene phenoxy species (see Fig. 1). Thiophene does not lower the barrier of this reaction: the presence of thiophene stabilizes the transition state only by 3 kJ/mol. Thiophene adsorbs on the phenoxy species. The physisorbtion energy is small $E_{ads} = -2$ kJ/mol. The transition state geometry of the methylation reaction of thiophene C_1 carbon atom is shown in Fig. 10. The activation energy barrier of this reaction is $E_{act} = 272$ kJ/mol with respect to toluene adsorbed on the cluster and thiophene energy. The reaction pathway is similar to the pathway already described in the alkylated thiophene part afterward (see Fig. 3). The computed activation barrier energy is $E_{act} = 277$ kJ/mol in the case of the alkylation on the C_2 position. With a difference of only 5 kJ/mol between the two activation barrier energies, there are no intrinsic differences toward a specific methylation position. When the opposite mechanism is considered (alkylation of benzene by a methyl-thiophene), the same conclusion can be drawn. We may assume that initial activation of methyl-1-thiophene is more favorable than the methyl-2-thiophene activation.

Except to C_1 and C_2 positions, the methylation of toluene on thiophene can also occur on the sulfur atom position (see Fig. 11). The activation energy barrier that is required to methylate thiophene on its sulfur atom is 272 kJ/mol with respect to adsorbed toluene and thiophene in gas phase. A charged species is formed (see Fig. 11). Despite the fact that this molecule is a charged species, one finds a stable (local) minimum. Its energy is 223 kJ/mol above the energy level of adsorbed toluene and thiophene. An activation energy barrier of only 34 kJ/mol is found for proton backdonation. Several reaction steps were investigated from this unstable species (viz. cracking (8c, 20) and disproportionation in the present study). The only disproportionation

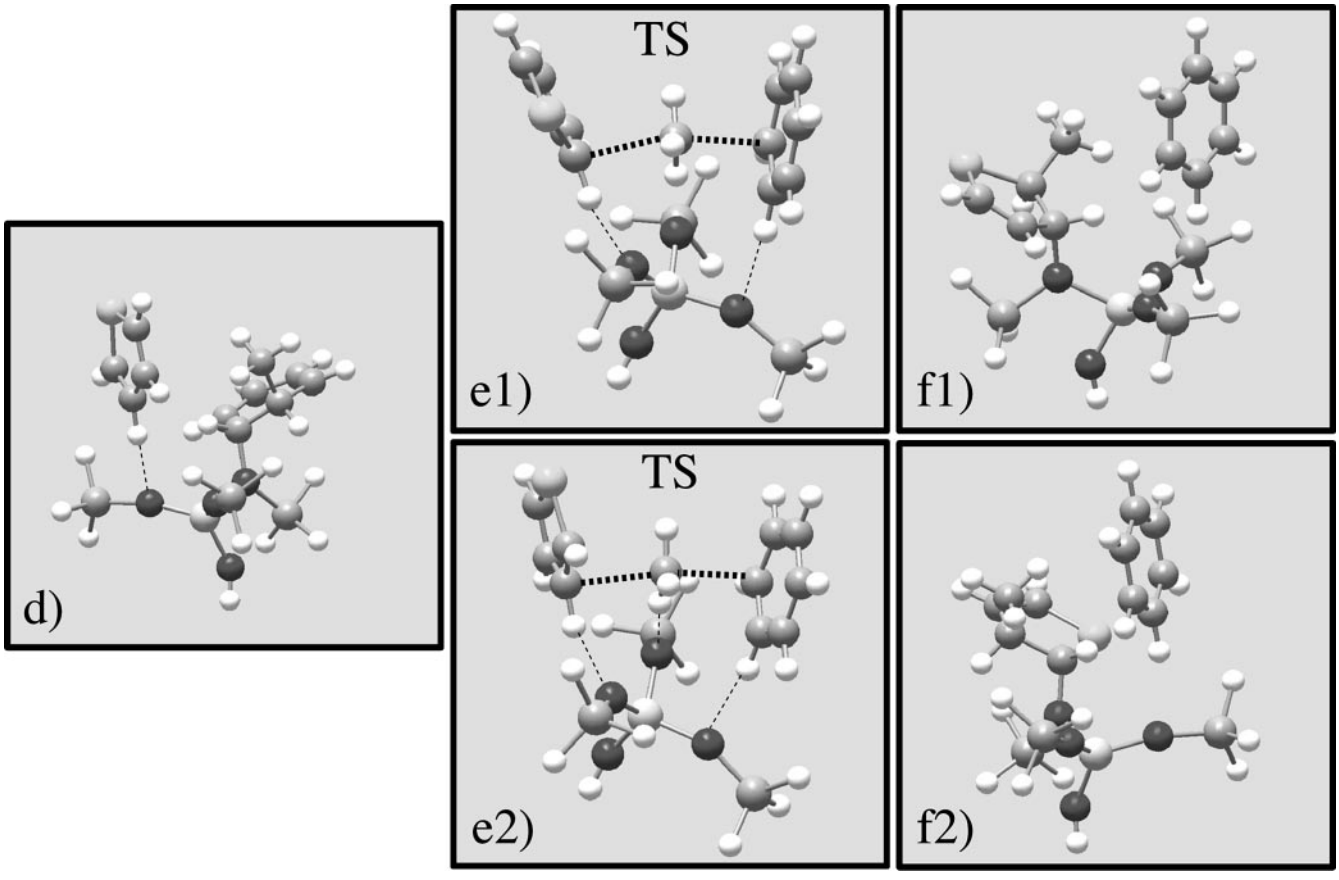

FIG. 10. Geometries of the intermediates and transition states for the mechanism of the direct mechanism transalkylation reaction between toluene and thiophene leading to the formation of benzene and methyl-1-thiophene (top) and benzene and methyl-2-thiophene (bottom).

reaction step that appears to be achievable is the donation of a methyl group to a Lewis basic oxygen atom of the negatively charged cluster (see Fig. 11). This reaction allows the formation of thiophene, benzene, and methyl alkoxy. It is possible to crack thiophene (20) or to alkylate another passing-by molecule from thiophene and methyl alkoxy (see Figs. 2 and 4).

All maximum activation energy barriers computed are within a span of 5 kJ/mol in the case of transalkylation reaction between thiophene and toluene. It is likely that all

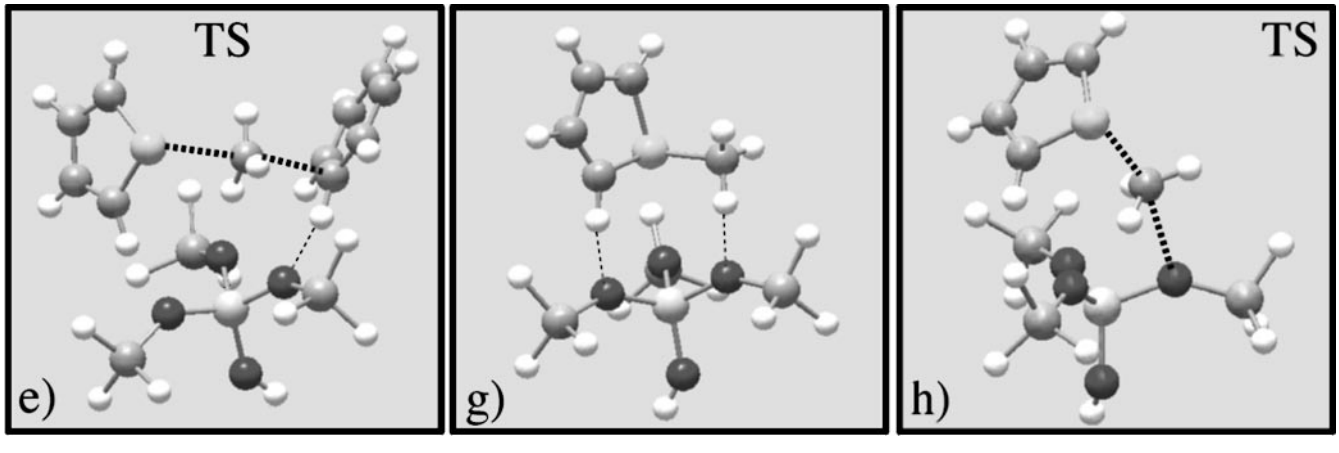

FIG. 11. Geometries of the (g) intermediate and (e and h) transition states for the mechanism of the direct mechanism transalkylation reaction between toluene and thiophene when alkylation occurs on the thiophene sulfur atom.

these reaction steps can occur in parallel and that selectivity toward one or the other product requires other factors, such as steric constraints and/or diffusivity.

4. CONCLUSION

We have investigated the reactions of isomerization of toluene, methyl-thiophene, and alkylated thiophene derivatives in this theoretical study. Moreover, transalkylation reactions of toluene–benzene and toluene–thiophene have been investigated.

Two different reaction pathways of intra-isomerization, viz. the shift 1–2 isomerization reaction and the disproportionation via a methyl alkoxy isomerization reaction, have been found (see Scheme 1). A phenoxy intermediate is involved in both of them. The highest activation energy barriers required to achieve toluene isomerization reaction are similar ($E_{act} \sim 280$ kJ/mol). A $\Delta E_{act} \sim 30$ kJ/mol is found for methyl-thiophene isomerization reaction. This would suggest that the shift 1–2 isomerization reaction is preferred ($E_{act} \sim 240$ and 270 kJ/mol for the shift 1–2 and disproportionation reactions, respectively). The shift isomerization reaction of 2MBT as well as for other benzothiophenic derivatives suggests that the reactivity of these species is closely related to the toluene derivative. Interestingly, it appears that large differences exist on the alkoxy intermediates. A proton attack on 2MBT leads to an alkoxy intermediate 15 kJ/mol more stable than in the case of the phenoxy intermediate, whereas the alkoxy intermediate formed after a proton attack on 3MBT gives an intermediate 25 kJ/mol less stable. One assumes, as steric constraints are similar on both thiophenophenoxy intermediates, that this energy difference originates from different sulfur atom positions as a function of the phenoxy bond.

Transalkylation reactions have also been analyzed. Two reaction mechanisms have been shown to occur. The first, the direct transalkylation reaction, requires an initiation step similar to the isomerization reaction (see Scheme 1). The highest activation energy does not show dependence whether transalkylation reaction occurs between toluene and benzene or toluene and thiophene. Furthermore, the alkylation reactions on a nonequivalent thiophenic position give the same activation energy. All highest activation energies of direct transalkylation reactions shown here are included within less than 3 around 275 kJ/mol. These values are less than 10 kJ/mol from activation energies of toluene isomerization reactions. When thiophene species are involved, only the proton attack differs. It appears easier than the activation of toluene ($\Delta E_{act} = 50$–80 kJ/mol).

Transalkylation reaction can proceed following another reaction pathway. This reaction involves a diphenylmethane intermediate and occurs via disproportionation reaction steps. The initiation step of this reaction is considerably more difficult than the initiation step of the direct transalkylation reaction ($E_{act} \sim 300$ vs 200 kJ/mol) but allows for the establishment of a less easily deactivated catalytic cycle ($E_{act} \sim 184$ vs 49 kJ/mol) (see Schemes 1 and 3). The activation barrier energy of the transalkylation step reaction is 30 kJ/mol lower than that of direct transalkylation.

This study has been realized using a small cluster approach method. Therefore, zeolite framework electrostatic contribution and steric constraints are missing. According to Sinclair *et al.* and Boronat *et al.* (13), it is likely that a uniform shift overestimation of the activation energies exists due to the absence of zeolite framework electrostatic contributions. Moreover, as a function of the available void cavity space within specific zeolite catalysts, bimolecular reaction steps or larger intermediates can be prevented to exist. However, despite the shortcuts of the cluster approach method, an analysis of the isomerization and transalkylation reactions of some aromatic species has been achieved. The deeper insight in these mechanisms can help both theoretical and experimental works. These results are extremely valuable as they allow for the establishment of a reactivity index of aromatic species activated by zeolitic Brønsted sites in the absence of zeolitic topology dependence.

ACKNOWLEDGMENTS

This work has been performed within the European Research Group "Ab Initio Molecular Dynamics Applied to Catalysis," supported by the Centre National de la Recherche Scientifique (CNRS), the Institut Français du Pétrole (IFP), and the TotalFina Raffinage Distributions company. X.R. and X.S. thank TotalFina Raffinage Distributions for the financial support. Computational resources were partly supplied by the Dutch National Computer Facilities.

REFERENCES

1. (a) Venuto, P. B., *Microporous Matter* **2**, 297 (1994); (b) Jacobs, P. A., and Martens, J. A., *in* "Introduction to Zeolite Science and Practice" (H. van Bekum, E. M Flaningen, and J. C. Jansen, Eds), Vol. 58, p. 445. Elsevier, Amsterdam, 1991.
2. Hölderich, W. F., and Van Bekkum, H., *in* "Introduction to Zeolite Science and Practice" (H. van Bekkum, E. M. Flaningen, and J. C. Jansen, Eds), Vol. 58, p. 631. Elsevier, Amsterdam, 1991.
3. Csicsery, S. M., *Zeolites* **4**, 202 (1984).
4. Blaszkowski, S. R., and Van Santen, R. A., *in* "Transition State Modeling for Catalysis" (D. G. Truhlar and K. Morokuma, Eds.), Chapter 24, ACS Symp. Ser. No. 721. Am. Chem. Soc., Washington, DC, 1999.
5. Landau, M. V., *Catal. Today* **36**, 393 (1997).
6. Geobaldo, F., Palomino, G. T., Bordiga, S., Zecchina, A., and Areán, C. O., *Phys. Chem. Chem. Phys.* **1**, 561 (1999).
7. (a) Van Santen, R. A., and Kramer, G. J., *Chem. Rev.* **95**, 637 (1995); (b) Sauer, J., *in* "Cluster Models for Surface and Bulk Phenomena: Proceedings of a NATO Advanced Research Workshop" (G. Pacchioni, P. S. Bagus, and F. Parmigiani, Eds.), p. 533. Plenum Press, London, 1992; (c) Van Santen, R. A., De Bruyn, D. P., Den Ouden, C. J. J., and Smit, B., *in* "Introduction to Zeolite Science and Practice" (H. van Bekkum, E. M. Flaningen, and J. C. Jansen, Eds.), Vol. 58, p. 317. Elsevier, Amsterdam, 1991.
8. (a) Beck, L. W., Xu, T., Nicholas, J. B., and Haw, J. F., *J. Am. Chem. Soc.* **117**, 11,594 (1995); (b) Corma, A., Sastre, G., and Viruela, P. M.,

J. Mol. Catal. A **100**, 75 (1995); (c) Saintigny, X., Van Santen, R. A., Clémendot, S., and Hutschka, F., *J. Catal.* **183**, 107 (1999); (d) Evleth, E. M., Kassab, E., Jessrich, H., Allavena, M., Montero, L., and Sierra, L. R., *J. Phys. Chem.* **100**, 11368 (1996); (e) Esteves, P. M., Nascimento, M. A. C., and Mota, C. J. A., *J. Phys. Chem. B* **103**, 10417 (1999); (f) Frash, M. V., Kazansky, V. B., Rigby, A. M., and Van Santen, R. A., *J. Phys. Chem. B* **101**, 5346 (1997).

9. (a) Kramer, G. J., De Man, A. J. M., and Van Santen, R. A., *J. Am. Chem. Soc.* **113**, 6435 (1991); (b) Kramer, G. J., and Van Santen, R. A., *J. Am. Chem. Soc.* **115**, 2887 (1993); (c) Rigby, A. M., Kramer, G. J., and Van Santen, R. A., *J. Catal.* **170**, 1 (1997).
10. (a) Van Santen, R. A., *J. Mol. Catal. A* **115**, 405 (1997); (b) Van Santen, R. A., *Catal. Today* **30**, 377 (1997); (c) Frash, M. V., and Van Santen, R. A., *Topics Catal.* **9**, 191 (1999); (d) Kazansky, V. B., *Catal. Today* **51**, 419 (1999).
11. (a) Sauer, J., *in* "Modeling of Structure and Reactivity in Zeolites" (C. R. A. Catlow, Ed.), p. 183. Academic Press, London, 1992; (b) Catlow, C. R. A., Ackermann, L., Bell, R. G., Corà, F., Gay, D. H., Nygren, M. A., Pereira, J. C., Sastre, G., Slater, B., and Sinclair, P. E., *Faraday Discuss.* **106**, 1 (1997); (c) Ugliengo, P., Civalleri, B., Zicovich-Wilson, C. M., and Dovesi, R., *Chem. Phys. Lett.* **318**, 247 (2000); (d) Brändle, M., and Sauer, J., *J. Am. Chem. Soc.* **120**, 1556 (1998); (e) Sastre, G., and Lewis, D. W., *J. Chem. Soc., Faraday Trans.* **94**, 3049 (1998).
12. (a) Sauer, J., Sierka, M., and Haase, F., *in* "Transition State Modeling for Catalysis" (D. G. Truhlar, and K. Morokuma, Eds.), p. 358. ACS Symp. Ser. No. 721. Am. Chem. Soc., Washington, DC, 1999; (b) Zygmunt, S. A., Curtiss, L. A., Zapol, P., and Iton, L. E., *J. Phys. Chem. B* **104**, 1944 (2000).
13. (a) Boronat, M., Viruela, P., and Corma, A., *J. Phys. Chem. A* **102**, 982 (1998). (b) Sinclair, P. E., De Vries, A., Sherwood, P., Catlow, C. R. A., and Van Santen, R. A., *J. Chem. Soc., Faraday Trans.* **94**, 3401 (1998).
14. Eichler, U., Brändle, M., and Sauer, J. *J. Phys. Chem. B* **101**, 10035 (1997).
15. Gorte, R. J., and White, D. *Microporous Mesoporous Mater.* **35–36**, 447 (2000).
16. Van Santen, R. A., and Rozanska, X., *in* "Advances in Chemical Enginering" Academic Press, to appear.
17. Frisch, M. J., Trucks, G. W., Schlegel, H. B., Scuseria, M. A., Robb, M. A., Cheeseman, J. R., Zakrzewski, V. G., Montgomery, J. A., Stratmann, R. E, Burant, J. C., Dapprich, S., Millam, J. M., Daniels, A. D., Kudin, K. N., Strain, M. C., Farkas, O., Tomasi, J., Barone, V., Cossi, M., Cammi, R., Mennucci, B., Pomelli, C., Adamo, C., Clifford, S., Ochterski, J., Petersson, G. A., Ayala, P. Y., Cui, Q., Morokuma, K., Malick, D. K., Rabuck, D. K., Raghavachari, K., Foresman, J. B., Cioslowski, J., Ortiz, J. V., Stefanov, B. B., Liu, G., Liashenko, A., Piskorz, P., Komaromi, I., Gomperts, R., Martin, R. L., Fox, D. J., Keith, T., Al-Laham, M. A., Peng, C. Y., Nanayakkara, A., Gonzales, C., Challacombe, M., Gill, P. M. W., Johnson, B. G., Chen, W., Wong, M. W., Andress, J. L., Head-Gordon, M., Replogle, E. S., and Pople, J. A., "Gaussian 98," revision A.1. Gaussian, Inc., Pittsburg, PA, 1998.
18. (a) Becke, A. D., *Phys. Rev. A* **38**, 3098 (1988); (b) Lee, C., Yang, W., and Parr, R. G., *Phys. Rev. B* **37**, 785 (1988); (c) Becke, A. D., *J. Chem. Phys.* **98**, 5648 (1993).
19. Zygmunt, S. A., Mueller, R. M., Curtiss, L. A., and Iton, L. E., *J. Mol. Struct.* **430**, 9 (1998).
20. Rozanska, X., Van Santen, R. A., and Hutschka, F., *J. Catal.* **200**, 79 (2001).
21. (a) Boys, S. F., and Bernardi, F., *Mol. Phys.* **19**, 553 (1970); (b) Van Duijneveldt, F. B., *in* "Molecular Interactions: From van der Waals to Strongly Bound Complexes" (S. Scheiner, Ed.), p. 81. Wiley, New York, 1997; (c) Lendvay, G., and Mayer, I., *Chem. Phys. Lett.* **297**, 365 (1998).
22. (a) Kumar, R., and Ratnasamy, P., *J. Catal.* **116**, 440 (1989); (b) Mirth, G., Cejka, J., and Lercher, J. A., *J. Catal.* **139**, 24 (1993).
23. (a) Cortes, A., and Corma, A., *J. Catal.* **51**, 338 (1978); (b) Young, L. B., Butter, S. A., and Kaeding, W. W., *J. Catal.* **76**, 418 (1982); (c) Beschmann, K., and Riekert, L., *J. Catal.* **141**, 548 (1993).
24. (a) Pérez-Pariente, J., Sastre, E., Fornés V., Martens, J. A., Jacobs, P. A., and Corma, A., *Appl. Catal.* **69**, 125 (1991); (b) Morin, S., Gnep, N. S., and Guisnet, M., *J. Catal.* **159**, 296 (1996).
25. (a) Olah, G. A., and Donovan, D. J., *J. Am. Chem. Soc.* **99**, 5026 (1977); (b) Olah, G. A., Prakash, G. K. S., and Sommer, J., "Superacids." Wiley, New York, 1985; (c) Olah, G. A., Prakash, G. K. S., Williams, R. E., Field, L. D., and Wade, K., "Hypercarbon Chemistry." Wiley, New York, 1987.
26. Gorte, R. J. *Catal. Lett.* **62**, 1 (1999).
27. (a) Haw, J. F., Richardson, B. R., Oshiro, I. S., Lazo, N. D., and Speed, J. A., *J. Am. Chem. Soc.* **111**, 2052 (1989); (b) Haw, J. F., Nicholas, J. B., Xu, T., Beck, L. W., and Ferguson, D. B., *Acc. Chem. Res.* **29**, 259 (1996).
28. (a) Parrillo, D. J., and Gorte, R. J., *J. Phys. Chem.* **97**, 8786 (1993); (b) Lee, C., Parrillo, D. J., Gorte, R. J., and Farneth, W. E., *J. Am. Chem. Soc.* **118**, 3262 (1996).
29. (a) De Man, A. J. M., Van Beest, B. W. H., Leslie, M., and Van Santen, R. A., *J. Phys. Chem.* **94**, 2524 (1990); (b) Schröder, K.-P., and Sauer, J., *J. Phys. Chem.* **100**, 11043 (1996); (c) Levien, L., Previtt, C. T., and Weider, D. J., *Am. Mineral.* **65**, 925 (1980).
30. (a) Lumpov, A. I., Mikheikin, I. D., Zhidomirov, G. M., and Kazansky, V. B., *Kinet. Katal.* **20**, 1979 (1979); (b) Senchenya, I. N., Mikheikin, I. D., Zhidomirov, G. M., and Kazansky, V. B., *Kinet. Katal.* **22**, 1174 (1980); (c) Senchenya, I. N., Mikheikin, I. D., Zhidomirov, G. M., and Kazansky, V. B., *Kinet. Katal.* **21**, 1184 (1980); (d) Senchenya, I. N., Mikheikin, I. D., Zhidomirov, G. M., and Kazansky, V. B., *Kinet. Katal.* **23**, 591 (1982).
31. (a) Kazansky, V. B., and Senchenya, I. N., *J. Catal.* **119**, 108 (1989); (b) Kramer, G. J., Van Santen, R. A., Emeis, C. A., and Nowak, A. K., *Nature* **363**, 529 (1993).
32. Michaud, P., Lemberton, J. L., and Pérot, G., *Appl. Catal. A* **169**, 343 (1998).
33. (a) Landau, M. V., Berger, D., and Herskowitz, M., *J. Catal.* **158**, 236 (1996); (b) Meille, V., Schulz, E., Lemaire, M., and Vrinat, M., *J. Catal.* **170**, 29 (1997); (c) Yu, S. Y., Li, W., and Iglesia, E., *J. Catal.* **187**, 257 (1999).
34. (a) Knudsen, K. G., Cooper, B. H., and Topsøe, H., *Appl. Catal. A* **189**, 205 (1999); (b) Singhal, G. H., Espino, R. L., and Sobel, J. E., *J. Catal.* **67**, 446 (1981); (c) Vasudevan, P. T., and Fierro, J. L. G., *Catal. Rev. Sci. Eng.* **38(2)**, 161 (1996).
35. Garcia, C. L., and Lercher, J. A., *J. Mol. Struct.* **293**, 235 (1993).
36. (a) Wang, I., Tsai, T.-C., and Huang, S.-T., *Ind. Eng. Chem. Res.* **29**, 2005 (1990); (b) Corma, A., and Sastre, E., *J. Catal.* **129**, 177 (1991); (c) Anderson, J. R., Dong, Q.-N., Chang, Y.-F., and Western, R. J., *J. Catal.* **127**, 113 (1991); (d) Corma, A., Llopis, F., and Monton, J. B., *J. Catal.* **140**, 384 (1993); (e) Pradhan, A. R., and Rao, B. S., *Appl. Catal. A* **106**, 143 (1993); (f) Forni, L., Cremona, G., Bellussi, G., Perego, C., and Pazzuconi, G., *Appl. Catal. A* **121**, 261 (1995); (g) Bandyopadhyay, R., Singh, P. S., and Shaikh, R. A., *Appl. Catal. A* **135**, 249 (1996); (h) Takeuchi, G., Shimoura, Y., and Hara, T., *Appl. Catal. A* **137**, 87 (1996); (i) Bandyopadhyay, R., Singh, P. S., and Rao, B. S., *React. Kinet. Catal. Lett.* **60**, 171 (1997); (j) Halgeri, A. B., and Das, J., *Appl. Catal. A* **181**, 347 (1999).
37. Tsai, T.-C., Liu, S.-B., and Wang, I., *Appl. Catal. A* **181**, 355 (1999).
38. Guisnet, M., Gnep, N. S., and Morin, S., *Microporous Mesoporous Mater.* **35**–**36**, 47 (2000).
39. Weitkamp, J., Raichle, A., Traa, Y., Rupp, M., and Fuder, F., *Chem. Comm.* **5**, 403 (2000).